

## Complexes of tetracyanobiimidazole—V. Self-association of Ir(I) complex anions

MILTON TAMRES,\* O. H. BAILEY, J. E. ANDERSON and P. G. RASMUSSEN\*  
Department of Chemistry, University of Michigan, Ann Arbor, Michigan 48109, U.S.A.

(Received 27 September 1985; in final form 13 December 1985; accepted 13 December 1985)

**Abstract**—The self-association of the planar anion  $[\text{Ir}(\text{CO})_2\text{Tcbiim}]^-$  where  $\text{H}_2\text{Tcbiim}$  is 4,4',5,5'-tetracyano-2,2'-biimidazole has been studied in acetonitrile solution by analysis of the charge-transfer spectra. At low concentrations ( $\sim 10^{-5}$  M) monomer units prevail. At intermediate concentrations ( $\sim 10^{-3}$  M) dimerization is evident and a very strong ( $\epsilon = 18\,500\text{ M}^{-1}\text{ cm}^{-1}$ ) new absorption appears at 475 nm. A novel procedure was used to obtain this value and to estimate the equilibrium constant for dimerization,  $13.2\text{ M}^{-1}$  at 24.4°C. From the temperature dependence of the spectra,  $\Delta H$  is calculated to be  $-28$  to  $-30\text{ kJ M}^{-1}$ . At higher concentrations ( $\sim 10^{-2}$  M) spectral changes consistent with further oligomerization are observed.

### INTRODUCTION

This research is part of the planned synthesis of one dimensional metal chain complexes based on the ligand 4,4',5,5'-tetracyano-2,2'-biimidazole ( $\text{H}_2\text{Tcbiim}$ ) [1]. As the dianion,  $\text{Tcbiim}^{2-}$  is a planar, weak pi-acid molecule. It has the ability to act as a bridging and non-bridging ligand, and has been observed to be four, three and two coordinate with a number of different metals [2–6] including Ir and Rh [7, 8]. The planarity of  $\text{Tcbiim}^{2-}$  allows metal–metal interactions to occur in Ir(I) square planar complexes. The Ir(I) salts with the general formula  $\text{M}[\text{Ir}(\text{CO})_2\text{Tcbiim}]$  have very interesting properties. The solid materials have a variety of colors which are cation dependent. The  $\text{NEt}_4^+$  salt is bright red, while the  $\text{Na}^+$  salt is dark blue, for example. The crystal structure of the  $\text{NEt}_4^+$  salt showed that this compound has a tendency to form dimers in the solid state, but that the dimers formed a slip stack as shown in Fig. 1.

In this paper, a new system of oligomers is identified in acetonitrile solution and their charge-transfer spectra and equilibria are described. The present work uses a novel procedure to obtain spectral and thermodynamic properties, and extends the earlier work on related compounds by OLMSTEAD and BALCH [9], GEOFFROY *et al.* [10] and SIGAL and GRAY [11] who have studied in some detail the tendencies of Rh(I) and Ir(I) complexes to oligomerize in solution. The field has been recently reviewed by BALCH [12].

### EXPERIMENTAL

#### Physical measurements

Elemental analyses were performed by Spang Micro-analytical Laboratory, Eagle Harbor, MI or at Galbraith Laboratories, Knoxville, TN, USA. Vis-u.v. spectra were obtained with a Cary 14 recording spectrophotometer, at a scan rate of 25 Å/s. To avoid a potential error due to time lag in pen response, all the absorbance data in the tables were obtained at fixed wavelength settings. Temperature regu-

lation was achieved by means of a constant temperature circulator (Haake FK 10) which pumped a 1:1 mixture by volume of ethylene glycol–water through a Varian thermostatable cell jacket around the cell compartments. The temperature was controlled to  $\pm 0.10^\circ\text{C}$  by fixed setting mercury regulators (H–B Inst. Co.) [13]. At low temperatures dry air was passed through the cell housing to prevent fogging. Matched ground-glass-stoppered quartz cells (Beckman Co.) with different path lengths ranging from 0.00904 to 10.02 cm were used with additional rubber caps to prevent acetonitrile evaporation. Cell lengths were calibrated using standard solutions of iodine in *n*-heptane using the band at 520 nm ( $\epsilon = 918\text{ M}^{-1}\text{ cm}^{-1}$ ) [14]. In all cases pure solvent was used as the reference.

All stock and sample solutions were prepared by weight. Since the solutions were quite dilute, the concentrations at any temperature were calculated from the density of pure acetonitrile [15]. In the temperature dependent studies, the

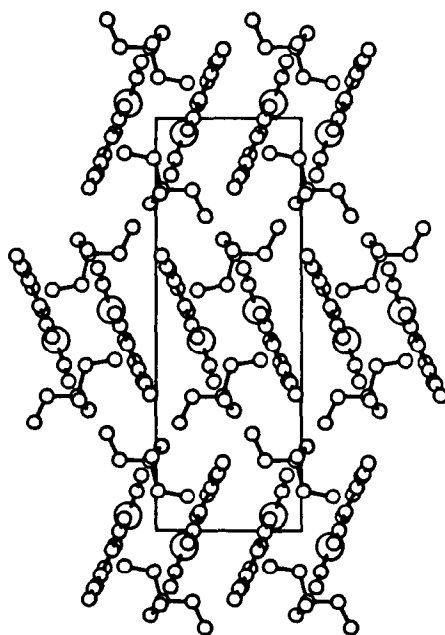


Fig. 1. View down the *b* axis of  $\text{Et}_4\text{N}[\text{Ir}(\text{CO})_2\text{Tcbiim}]$ . Ir–Ir distances are 3.18 and 4.72 Å.

\* Authors to whom correspondence should be addressed.

initial temperature was always rerun at the end of the experiment. No significant change in absorbance was found, demonstrating the absence of irreversible reactions and the stability of the base line with temperature.\*

#### Reagents

The ligand  $H_2Tcbiim$  and the compound  $M[Ir(CO)_2Tcbiim]$  where  $M$  is a simple cation were prepared by methods previously described [1, 7]. Acetonitrile (Fisher) was distilled from calcium hydride and stored under nitrogen. The reagents were exposed to the atmosphere in weighing to make up stock solutions and in filling the optical cells. They were found to be stable after this exposure for several days.

#### DISCUSSION

Figure 2 shows the visible spectrum of  $Na[Ir(CO)_2Tcbiim] \cdot 2H_2O$  in acetonitrile solution: cell path = 10.02 cm; (1)  $[Ir(CO)_2Tcbiim]^- = 3.293 \times 10^{-5} M$  at  $24.4^\circ C$ ; (2)  $[Ir(CO)_2Tcbiim]^- = 3.383 \times 10^{-5} M$  at  $4.7^\circ C$ . The difference in concentration at the two temperatures is based on the difference in density of the  $CH_3CN$  pure solvent at these temperatures. At this extreme dilution the two overlapping bands at 372 nm and 410 nm are attributed to monomer only. (There is a third, more intense band in the u.v. region at 318 nm.) There is no evidence for the presence of a dimeric species. First, there is no absorbance in the dimer band region (Fig. 3) and,

second, there is an *increase* in monomer absorbance with decrease in temperature (Fig. 2). The latter is opposite in direction to dimer formation. The increased absorbance at lower temperature (about 4%) can be accounted for largely by the change in density (about 3%). From the absorbance, concentration and cell path data, the molar absorbances of the monomeric bands at 372 and 410 nm can be determined fairly precisely: (1) at  $24.4^\circ C$ ,  $\epsilon_{372} = 2900 M^{-1} cm^{-1}$ ,  $\epsilon_{410} = 654 M^{-1} cm^{-1}$ ; (2) at  $4.7^\circ C$ ,  $\epsilon_{372} = 2950 M^{-1} cm^{-1}$ ,  $\epsilon_{410} = 661 M^{-1} cm^{-1}$ .

Figure 3 shows the visible spectrum of a  $10^{-3} M$  solution of  $[Ir(CO)_2Tcbiim]^-$  in  $CH_3CN$  over the temperature range  $4.7$ – $32.2^\circ C$  using a cell path of 0.4966 cm. At this concentration, a new band appears near 475 nm. For the several concentrations studied, a plot of  $A_{372}^2$  vs  $A_{475}$  for a common path length is linear (see Eqn. 5), indicating that the band corresponds to the formation of a dimer. The band increases in intensity with decreasing temperature, as expected for a dimerization process. The overlap of the dimer band with the monomer band at 410 nm causes the latter band to increase in absorbance with decrease in temperature. Apparently, the dimer band does not overlap with the monomer band at 372 nm. The near constancy in absorbance of the monomeric band at 372 nm with decrease in temperature implies that the loss in monomer concentration to form dimer is offset by the increase in density of the solution. The offset is not due to the absorbance tail of the dimer band. This can be seen in the spectrum at higher concentration

\* Absorbance data are presented in Tables 2–7, available as supplementary data from the Editorial Office.

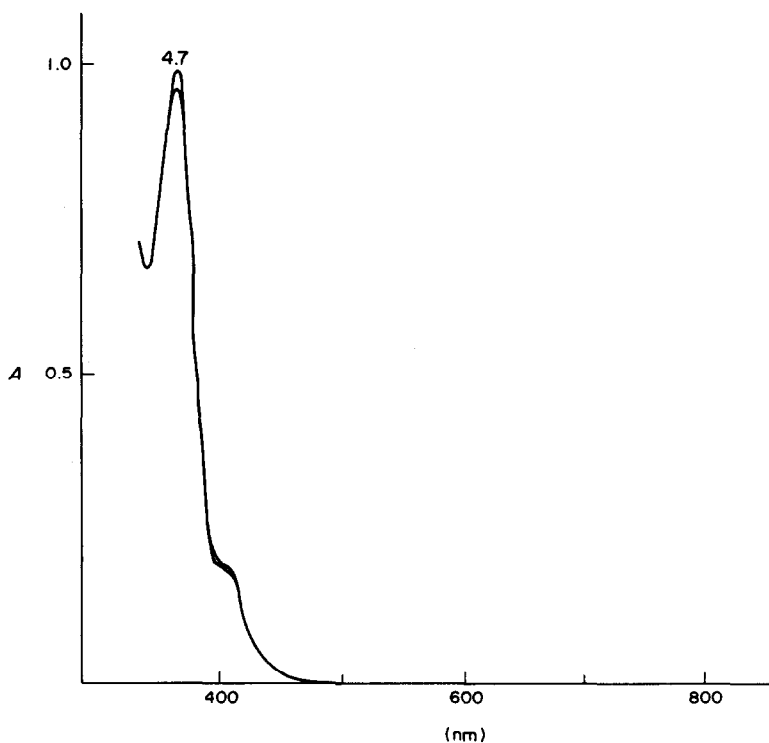


Fig. 2. Visible spectra of  $3.3 \times 10^{-5} M Na[Ir(CO)_2Tcbiim]$  in acetonitrile:  $T = 4.7$  and  $24.4^\circ C$ , path length = 10.02 cm.

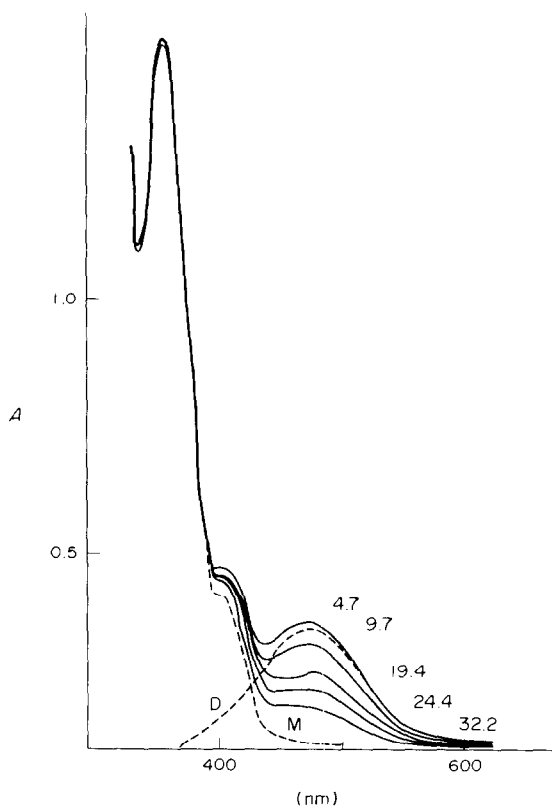
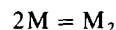


Fig. 3. Visible spectra of  $1.0 \times 10^{-3}$  M  $\text{Na}[\text{Ir}(\text{CO})_2\text{Tcbiim}]$  in acetonitrile:  $T = 4.7, 9.7, 19.4, 24.4$  and  $32.2^\circ\text{C}$ ; path length =  $0.4966$  cm. Dashed curves are the resolved bands of the monomer M and dimer D at  $4.7^\circ\text{C}$ .

(Fig. 4) where the monomer absorbance at  $372$  nm decreases with decreasing temperature.

Assuming negligible overlap of the dimer band with the monomer band at  $372$  nm, the monomer and dimer bands in Fig. 3 can be resolved. The concentration of the monomer in Fig. 3 is obtained directly from the absorbance at  $372$  nm (since  $\epsilon_{372}$  and cell path are known). The relative absorbances Fig. 2 give directly the ratio of the molar absorbance of the monomer at  $372$  nm with that at any other wavelength nm i.e.  $\epsilon_{372}/\epsilon_{nm}$  (Table 2). Applying these data in Fig. 3 gives the contribution of the monomer band at  $4.7^\circ\text{C}$ . Subtraction of the monomer band from the composite band at  $4.7^\circ\text{C}$  gives the dimer band (Fig. 3 and Table 3). For dimer formation:



where  $M_2$  is dimer (D); the equilibrium constant is:

$$K_D = \frac{[M_2]}{[M]^2} \quad (1)$$

In terms of initial monomer concentration  $[M]_0$

$$K_D = \frac{[M_2]}{([M]_0 - 2M_2)^2} \quad (2)$$

The total absorbance ( $A_T$ ) is the sum of that due to monomer ( $A_M$ ) and dimer ( $A_D$ )

$$A_T = A_M + A_D = l\epsilon_M[M] + l\epsilon_D[M_2]$$

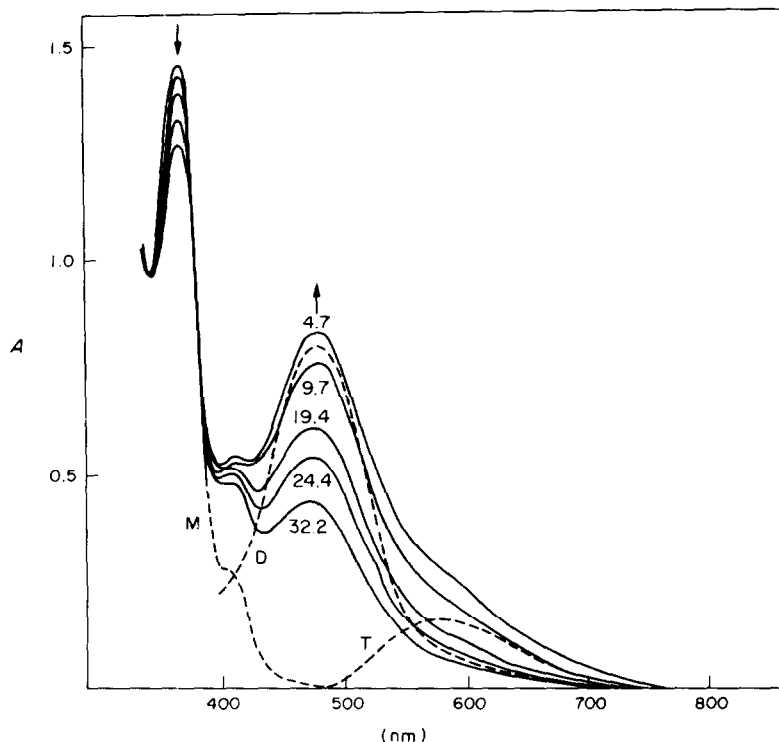


Fig. 4. Visible spectra of  $5.0 \times 10^{-3}$  M  $\text{Et}_4\text{M}[\text{Ir}(\text{CO})_2\text{Tcbiim}]$  in acetonitrile:  $T = 4.7, 9.7, 19.4, 24.4$  and  $32.2^\circ\text{C}$ ; path length =  $0.0983$  cm. Dashed curves are the resolved bands of the monomer M, dimer D and trimer T (plus higher oligomers).

or from Eqn. (2):

$$A_T - l\epsilon_M[M] = lK_D\epsilon_D([M]_0 - 2M_2)^2 \quad (3)$$

It has been shown, at a wavelength where  $\epsilon_D \gg \epsilon_M$ , that Eqn. (3) becomes [16]:

$$\frac{l[M]_0^2}{A_T - A_0} = \frac{1}{K_D\epsilon_D} + \frac{4[M]_0}{\epsilon_D} - \frac{4(A_T - A_0)}{l\epsilon_D^2} \quad (4)$$

where  $A_0 = l\epsilon_M[M]_0$ . Usually the last term in Eqn. (4) is small and can be omitted. Plotting the spectral data for several concentrations of  $[M]_0$  according to Eqn. (4) allows determination of  $K_D$  and  $\epsilon_D$  from the slope and intercept. Limitations of using this procedure have been discussed [17, 18]. Indeed, this procedure is not valid at all in the present study, in which  $K$  is relatively small, the concentrations are low due to limited solubility and the formation of oligomers is possible.

In principle, having resolved the monomer and dimer bands and knowing the characteristics of the monomer band, it should be possible to calculate the dimer concentration and, hence,  $K_D$ . This involves determining a small difference between two large numbers at two concentrations, making the results unreliable. (The dimer concentration sometimes comes out to be negative.) This difficulty is circumvented by noting the following: the absorbance data at 372 nm in Fig. 3 indicate very little dimer association, i.e. the  $\epsilon_{372}$  value is within a few per cent of that in Fig. 2. The dimer band at 475 nm in Fig. 3 shows an increase in dimer formation with decrease in temperature, but the monomer band at 372 nm remains constant over the temperature range. This means that the term  $([M]_0 - 2M_2)$  in Eqn. (2) has the same value for all five curves in Fig. 3. Equating, for example, the data for curve 5:  $[M_0] = 1.0219 \times 10^{-3}$ ;  $[M_2] = 0.256/\epsilon_D(0.4966)$ ; and curve 1:  $[M_0] = 0.9827 \times 10^{-3}$ ;  $[M_2] = 0.079/\epsilon_D(0.4966)$ ; gives directly the value for  $\epsilon = 18\,200 \text{ M}^{-1} \text{ cm}^{-1}$  (assuming constancy with temperature). The average for all combinations is  $18\,500 \pm 3500 \text{ M}^{-1} \text{ cm}^{-1}$ .  $M_2$  can be calculated at each temperature, and  $K_D$  can be obtained directly from Eqn. (2). The data are summarized in Table 1.

The study of the temperature dependence of the absorbance in Fig. 3 allows determination of the

enthalpy of dimer formation. Combining Beer's law

$$[M_2] = A_D/\epsilon_D l$$

$$[M] = A_M/\epsilon_M l$$

and Eqn. (1) gives:

$$\frac{A_D}{A_M^2} = \frac{K_D\epsilon_D}{\epsilon_M^2 l} \quad (5)$$

Assuming  $\epsilon_D$  and  $\epsilon_M$  are essentially temperature independent:

$$\frac{d \log (A_D/A_M^2)}{d(1/T)} = \frac{d \log K_D}{d(1/T)}$$

Thus a plot of  $\log (A_D/A_M^2)$  vs  $1/T$  is equivalent to plotting  $\log K_D$  vs  $1/T$ . The slope of this plot equals  $-\Delta H/2.303R$ . The plots in Fig. 5 are for the monomeric absorbance data at 372 nm and the dimeric

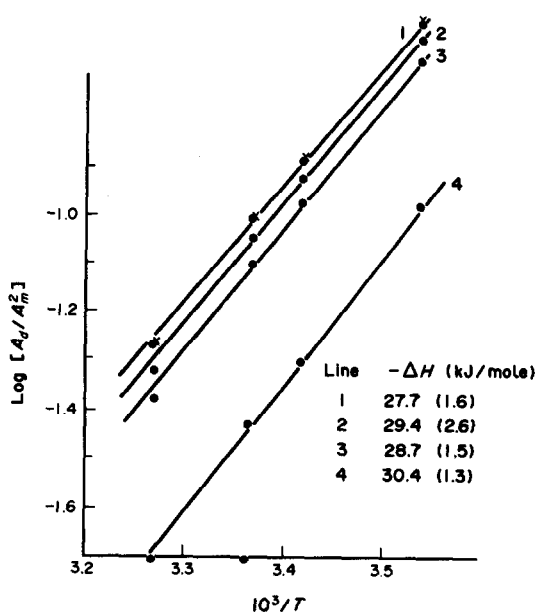


Fig. 5. Plots to determine the heat of dimerization of the  $[\text{Ir}(\text{CO})_2\text{Tcbium}]^-$  ion in acetonitrile:  $\times = \text{Na}^+$  salt;  $\bullet = \text{Et}_4\text{N}^+$  salt. Monomer band at 372 nm and dimer band at (1) 475 nm, (2) 490 nm, (3) 500 nm, (4) 525 nm in parentheses 95% level. Error limits in parentheses 95% level.

Table 1. Evaluation of  $K_D$  and  $K_D\epsilon_D$  from the absorption band at 475 nm in Fig. 3

Curve	$t$ (°C)	$[M]_0^* \times 10^3$ (mol l <sup>-1</sup> )	Abs $\dagger$ ‡ (475 nm)	$[M_2] \times 10^5$ (mol l <sup>-1</sup> )	$K_D$ (l mol <sup>-1</sup> )	$K_D\epsilon_D$ § (l <sup>2</sup> mol <sup>-2</sup> cm <sup>-1</sup> )
1	32.2	0.9827	0.079	0.860	9.2	170 000
2	24.4	0.9946	0.114	1.241	13.2	244 000
3	19.4	1.0016	0.141	1.536	16.3	302 000
4	9.7	1.0150	0.211	2.298	24.5	453 000
5	4.7	1.0219	0.256	2.789	29.9	553 000

\*Differences due to density change.

†Cell path = 0.4966 cm.

‡Differs from the data in Table 4 by 0.015 absorbance unit, attributed to slight monomer contribution.

§Based on  $\epsilon_D = 18\,500 \text{ l mol}^{-1} \text{ cm}^{-1}$  at 475 nm for this temperature range.

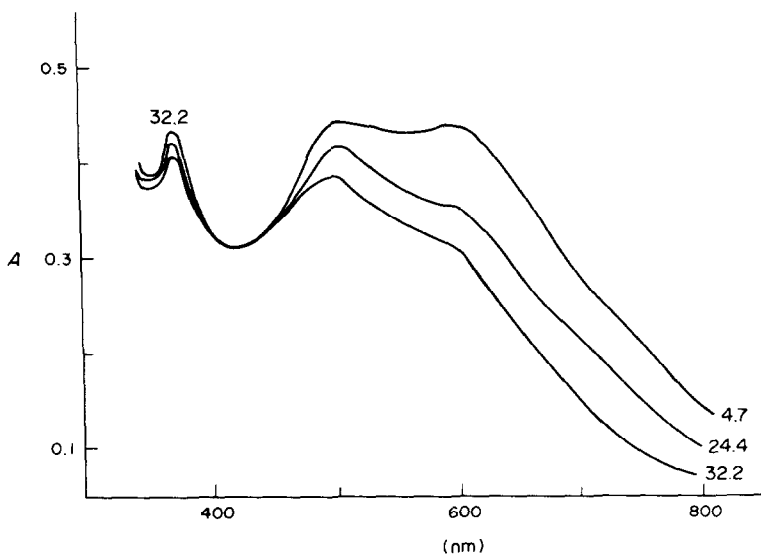


Fig. 6. Visible spectra of  $23 \times 10^{-3}$  M  $\text{Na}[\text{Ir}(\text{CO})_2\text{Tcbiim}]$  in acetonitrile:  $T = 4.7, 24.4$  and  $32.2^\circ\text{C}$ ; path length =  $0.00904$  cm.

absorbance data at (1) 475 nm, (2) 490 nm, (3) 500 nm and (4) 525 nm (Table 4). The figure shows that the data for the  $\text{Na}^+$  and  $\text{Et}_4\text{N}^+$  salts are identical. Regression analysis of the data in Fig. 5 gives the results listed in the insert (and in Table 5). In principle, the value for  $\Delta H$  should remain the same regardless of the wavelength of the dimer band selected for the calculation. A small, but systematic, increase in  $\Delta H$  is found in going from the value at 475 nm to that at 525 nm. Since the dimer absorbances are rather small, the trend may be fortuitous. Another possibility is a very small overlapping contribution of the trimer band with the dimer band. Generally, charge-transfer bands are asymmetric with greater breadth on the high frequency side [19], whereas the observed shape of the dimer band in Fig. 2 is skewed slightly the other way. However, the contribution of the trimer must be quite small as evidenced by the dimer band half-width of  $4400\text{ cm}^{-1}$ , which is typical for charge-transfer spectra [20]. The above procedure to determine  $\Delta H$  directly from absorbance data is free of approximations or of precise knowledge of the concentration. Usually, there is greater error associated with determining individual values of  $K$ . As a check of the data in Table 1, a plot of  $\ln K_D$  against  $1/T$  gave a good straight line. From the slope, the value of  $30.1 \pm 2.9\text{ kJ mol}^{-1}$  for  $-\Delta H$  dimerization was obtained. This is in the range of  $28\text{--}30\text{ kJ mol}^{-1}$  found by the other procedure.

The spectrum in Fig. 4, compared with that in Fig. 3, is for a five-fold increase in concentration of the complex and a five-fold decrease in cell path. The absorbance data of Fig. 4 are listed in Table 6. The dimer band at 475 nm is greatly enhanced, while the monomer band at 372 nm is diminished. A new band appears at about 600 nm attributed to a trimer. Resolution of Fig. 4 at  $4.7^\circ\text{C}$  into component bands (Table 7) was based on the assumption that the

absorbance at 372 nm is due to monomer only and that at 475 nm is due to dimer only. This procedure of resolving the bands gave the same dimer band half-width in Fig. 3 as in Fig. 2. Having resolved monomer and dimer bands, and knowing their respective extinction coefficients and cell paths,  $K_D$  can be calculated directly from Eqn. (1). The results are as follows:  $K_D$ ,  $1\text{ mol}^{-1}$  (at  $t^\circ\text{C}$ ) =  $9.9(32.2)$ ;  $12.9(24.4)$ ;  $15.0(19.4)$ ;  $20.8(9.7)$ ;  $25.1(4.7)$ . These data are within about 20% of those in Table 1 and give a reasonable check considering the difficulties of quantitative band resolution. In fact, the attempt to estimate a "trimer" concentration from  $[\text{M}_3] = 1/3([\text{M}_0] - [\text{M}] - 2[\text{M}_2])$  gave negative concentrations at the higher temperatures, thereby precluding determination of higher equilibria.

The residual band at longer wavelengths in Fig. 4 is markedly skewed, suggesting contribution from oligomers higher than the trimer. The highest concentration studied (Fig. 6),  $\sim 23 \times 10^{-3}$  M, is at about the limit of solubility of  $\text{Na}[\text{Ir}(\text{CO})_2\text{Tcbiim}]$  in acetonitrile. The very broad absorbances in the range  $600\text{--}700\text{ nm}$  give direct evidence for the presence of higher oligomers.

*Acknowledgements*—The authors are grateful to Professor ANDREAS LUDI, Bern, Switzerland for helpful discussions, and for support from NSF INT-8304329 for international cooperation. P.G.R. acknowledges support from the donors of the Petroleum Research Fund administered by the American Chemical Society.

#### REFERENCES

- [1] P. G. RASMUSSEN, R. L. HOUGH, J. E. ANDERSON, O. H. BAILEY and J. C. BAYON, *J. Am. chem. Soc.* **104**, 6155 (1982).
- [2] P. G. RASMUSSEN and J. E. ANDERSON, *Polyhedron* **2**, 547 (1983).
- [3] P. G. RASMUSSEN, J. E. ANDERSON and J. C. BAYON *Inorg. chim. Acta* **87**, 159–164 (1984).

- [4] P. G. RASMUSSEN, O. H. BAILEY and J. C. BAYON, *Inorg. chim. Acta* **86**, 107 (1984).
- [5] P. G. RASMUSSEN and J. C. BAYON, *Inorg. chim. Acta* **81**, L15 (1984).
- [6] P. G. RASMUSSEN, J. E. ANDERSON, O. H. BAILEY, M. TAMRES and J. C. BAYON, *J. Am. chem. Soc.* **107**, 279 (1985).
- [7] P. G. RASMUSSEN, O. H. BAILEY and J. C. BAYON *Inorg. Chem.* **23**, 338 (1984).
- [8] P. G. RASMUSSEN, O. H. BAILEY, J. C. BAYON and W. M. BUTLER, *Inorg. Chem.* **23**, 343 (1984).
- [9] M. M. OLMSTEAD and A. L. BALCH, *J. Organometal. Chem.* **148**, C15 (1978).
- [10] G. L. GEOFFROY, M. G. BRADLEY and M. E. KEENEY, *Ann. N.Y. Acad. Sci.* **313**, 588 (1978).
- [11] I. S. SIGAL and H. B. GRAY, *J. Am. chem. Soc.* **103**, 2220 (1981).
- [12] A. L. BALCH, in *Extended Linear Chain Compounds*, Vol. 1 (edited by J. MILLER). Plenum Press, New York (1980).
- [13] H. C. TSE and M. TAMRES, *J. phys. Chem.* **81**, 1367 (1977).
- [14] J. D. CHILDS, Ph.D. Thesis, University of Oklahoma, Norman, OK (1971).
- [15] J. TIMMERMANS, *Physico-chemical Constants of Pure Organic Compounds*, Vol. II, p. 343. Elsevier, New York (1965).
- [16] M. TAMRES, W. K. DUERKSEN and J. M. GOODENOW, *J. phys. Chem.* **72**, 966 (1968).
- [17] W. B. PERSON, *J. Am. chem. Soc.* **87**, 167 (1965).
- [18] M. TAMRES, *J. phys. Chem.* **65**, 654 (1961).
- [19] R. S. MULLIKEN and W. B. PERSON, *Molecular Complexes. A Lecture & Reprint Volume*, p. 113. Wiley-Interscience, New York (1969).
- [20] M. TAMRES, in *Molecular Complexes*, Vol. 1, Ch. 2 (edited by R. FOSTER). Paul Elek, London (1973).